Rydberg Atom Entanglements in the Weak Coupling Regime

Hanlae Jo, Yunheung Song, Minhyuk Kim, and Jaewook Ahn*
Department of Physics, KAIST, Daejeon 305-701, Korea

(Received 1 August 2019; published 24 January 2020)

We present an entanglement scheme for Rydberg atoms using the van der Waals interaction phase induced by Ramsey-type pulsed interactions. This scheme realizes not only controlled phase operations between atoms at a distance larger than Rydberg blockade distance, but also various counterintuitive entanglement examples, including two-atom entanglement in the presence of a closer third atom and W-state generation for three partially blockaded atoms. Experimental realization is conducted with single rubidium atoms in optical tweezer dipole traps, to demonstrate the proposed entanglement generations with an entanglement fidelity of $\mathcal{F} = 0.59 \pm 0.11$.

DOI: 10.1103/PhysRevLett.124.033603

Quantum entanglement is one of the most bizarre and intriguing natures of quantum mechanics [1], which plays an important role in understanding the physics of quantum many-body systems [2–4] and also empowering various quantum applications such as quantum computing [5], quantum sensing [6], and quantum communications [7]. Currently, there is a strong interest for the generation, manipulation, and detection of quantum entanglements, being investigated in many physical systems including photons [8], atoms [9–12], ions [13], and solid-state systems such as superconducting circuits [14] and defective diamonds [15]. However, in most of the systems, entanglement skills need further improvements even to operate a small-scale quantum computer.

Entanglement of arbitrary qubit pairs, especially ones that are not in the proximity, is of particular importance for scalable quantum systems of good connectivity. Although it has been achieved, for example, in trapped ions by common-mode motion [16,17] and in superconducting circuits by a cavity bus [18], it has not been realized in most other systems including Rydberg-atom systems, of particular relevance in the context of the present work. The widely used entanglement scheme of Rydberg atom systems [9–12] is based on the Rydberg-blockade effect [19], which prohibits double excitation to a Rydberg energy state among atoms closer than the blockade radius $r_b = (C_6/\Omega)^{1/6}$ defined by Rabi frequency Ω and van der Waals interaction strength C_6. In this scheme (model B of Ref. [19]), therefore, all and only the pairs of atoms within r_b are to be simultaneously entangled, making these entanglements short-ranged ($d < r_b$).

In this Letter, we experimentally demonstrate atom-pair entanglement in the weak-coupling regime ($d > r_b$), which is closely related to model A in Ref. [19]. With this, long-ranged atom entanglements are enabled beyond the Rydberg blockade distance, even in the presence of closer atoms that are to be left unentangled. In the weak-coupling regime, the doubly excited Rydberg state of two atoms separated by a distance d gains interaction phase $\alpha = \tau C_6/d^6$, i.e., $|11\rangle \rightarrow \exp(-i\alpha)|11\rangle$, during an interaction time τ, where the pseudospin states $|1\rangle$ and $|0\rangle$ represent the Rydberg and ground states, respectively. So, a pair of atoms separated by $d_\pi = (\tau C_6/\pi)^{1/6}$ undergoes a controlled π-phase gate and $d_{2\pi} = (\tau C_6/2\pi)^{1/6}$ a controlled 2π-phase gate that is the Null gate. Utilizing this interaction phase, we present three entanglement examples: First, we generate the entanglement of two atoms at a distance beyond the blockade radius. Second, we use three atoms in the linear configuration, ABC, with $d_{AB} > d_{BC} > r_b$, and operate the controlled π-phase gate only on the AB pair, while the closer pair BC is left separable. Third, we produce the W state of three partially blockaded atoms using a two-pulse coherent control scheme.

We use Ramsey interferometry to generate and measure the two-atom entanglements in the weak coupling regime. As in Fig. 1(a), two resonant $\pi/2$ pulses time separated by τ interact with two atoms A and B separated at a distance d ($>r_b$) and initially in the ground state $|00\rangle$. The first Ramsey pulse rotates each atom about the y axis to prepare the superposition state $|{+}{+}\rangle$, in which $|+\rangle = (|0\rangle + |1\rangle)/\sqrt{2}$ of each atom. During the time interval τ, van der Waals interaction induces a phase factor $e^{-i\alpha}$ to the doubly excited state $|11\rangle$. Finally, the second Ramsey pulse rotates each atom by $\pi/2$ about the axis $\hat{n}_\phi = \cos\phi\hat{y} - \sin\phi\hat{x}$, where ϕ is the laser phase that fine controls the azimuthal angle of the Bloch vector with respect to the y axis. The given optical process is described by the following unitary operation defined for the two-qubit Hilbert space as

$$U(\alpha,\phi) = R^{\pi/2}_{\hat{n}_\phi,A} \otimes R^{\pi/2}_{\hat{n}_\phi,B} e^{-in_A n_B \alpha} R^{\pi/2}_{\hat{y},A} \otimes R^{\pi/2}_{\hat{y},B}, \quad (1)$$

where $R^{\pi/2}_{\hat{y}}$ and $R^{\pi/2}_{\hat{n}_\phi}$ are single-qubit $\pi/2$ rotations about the axes, $\hat{y}$ and $\hat{n}_\phi$, respectively; and $n_{A,B}$ are the excitation

 © 2020 American Physical Society

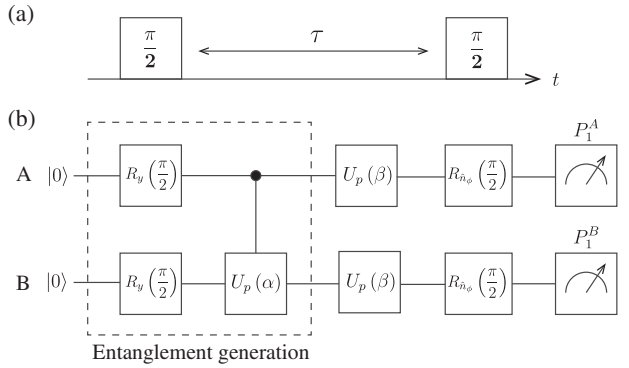

FIG. 1. (a) Ramsey-type double $\pi/2$ interactions. (b) Corresponding quantum circuit, in which two atoms A and B undergo the first Ramsey interaction $R_{\hat{y}}(\pi/2)$, controlled $U_p(\alpha = \tau C_6/d^6)$ phase gate, a residual local phase $U_p(\beta)$, and the second Ramsey $R_{\hat{n}_\phi}(\pi/2)$ fine controlled by laser phase ϕ.

number of the atoms. An equivalent quantum circuit is shown in Fig. 1(b), including an additional state-independent local phase β which will be explained in the experiment. After the entanglement generation (enclosed by a dashed box) the two-atom state evolves to

$$|\psi(\tau)\rangle = \frac{1}{2}(|00\rangle + |01\rangle + |10\rangle + e^{-i\alpha}|11\rangle), \qquad (2)$$

which is maximally entangled at $\alpha = (2n+1)\pi$, for an integer n, or loses entanglement at $\alpha = 2n\pi$. The resulting entanglement can be characterized by a Ramsey-type measurement [20] with the second $\pi/2$ pulse. As a function of the control phase ϕ, the probability of each atom, projected to $|1\rangle$, is given by

$$P_1^A = P_1^B = \frac{1}{2} + \frac{1}{2}\cos\left(\frac{\alpha}{2}\right)\cos\left(\frac{\alpha}{2} + \beta + \phi\right). \qquad (3)$$

So, the resulting fringe visibility, $\cos(\alpha/2)$, manifests the entanglement: maximal (minimal) visibility for no (maximal) entanglement.

Experiments were performed with an apparatus previously reported elsewhere [4,21,22]. In brief, we used optical tweezers to trap rubidium (^{87}Rb) single atoms and, with a 2-ms optical pumping, prepared them in the ground state $|0\rangle = |5S_{1/2}, F = 2, m_F = 2\rangle$. We then turned off the optical tweezers and excited the atoms to a Rydberg state $|1\rangle = |67S_{1/2}, J = 1/2, m_J = 1/2\rangle$, through the off-resonant intermediate state $|5P_{3/2}\rangle$, with counterpropagating 780-nm and 480-nm beams of σ^+ and σ^- polarizations, respectively. With $C_6 = 2\pi \times 513\ \mathrm{GHz}\,\mu\mathrm{m}^6$ [23], two-photon Rabi frequency $\Omega = 2\pi \times 0.83$ MHz gives the blockade radius of $r_b = 9.23\ \mu$m in the first two experiments. So, a time delay $\tau = 2.6\ \mu$s renders $d_\pi = 1.28 r_b$ for $\alpha = \pi$ and $d_{2\pi} = 1.14 r_b$ for $\alpha = 2\pi$. The Ramsey pulses were produced with an acousto-optic modulator by switching the 780-nm beam on and off twice, while the 480-nm beam was left on. The two-photon resonance was maintained with the laser-induced ac Stark shift, $\delta_{\mathrm{ac}} = 2.1$ MHz, taken into account. So, during the time interval, the excited state of each atom gained the phase $\beta = 2\pi \times \delta_{\mathrm{ac}}\tau$, while the doubly excited $|11\rangle$ state gained α, as in Eq. (2). After the interactions of the two $\pi/2$ pulses, the optical tweezers were turned back on to recapture the ground-state atoms, which were then recorded through 30-ms fluorescence imaging of the cyclic transition between $|5S_{1/2}, F = 2\rangle$ and $|5P_{3/2}, F' = 3\rangle$. We accumulated about 200–400 times of successful experiments to obtain P_1 (unsuccessful ones initially with an incomplete atom pair were all discarded), and repeated the entire process by varying the laser phase ϕ to obtain $P_1(\phi)$.

For a quantitative analysis, Monte Carlo numerical simulation was performed, taking the following experimental errors into account. (1) The Rabi frequency error mainly caused by beam pointing fluctuations was $\Delta\Omega/\Omega = 10\%$, estimated by Rabi measurements. (2) The atom temperature was $T = 22\ \mu$K, estimated by Ramsey and release-recapture [24] measurements. (3) State preparation and measurement errors were measured as the escape probability of ground-state atoms of 2% and the recapture probability of Rydberg-state atoms of 10%. (4) The excitation laser phase noise of $\Delta\phi = 0.2\pi$ (standard deviation) and (5) the distance error of about $\Delta d = 0.14\ \mu$m (standard deviation) were estimated through parameter adjustments in Monte Carlo simulation.

Figure 2 summarizes the result of the first experiment, atom-pair entanglements in the weak coupling regime. Two atoms A and B were placed at a distance of either $d_\pi = 1.28 r_b$ for maximal entanglement or $d_{2\pi} = 1.14 r_b$ for no entanglement, as shown in Fig. 2(a). Expected quantum trajectories, of each atom, are plotted on the Bloch sphere in Figs. 2(b) and 2(c), respectively. In the maximal entanglement case in Fig. 2(b), the quantum state of each atom A or B evolves from $|0\rangle$ to $|+\rangle$, due to the first Ramsey interaction, and then to the center of the Bloch sphere, driven by the van der Waals interaction of $\alpha = \pi$, so the second Ramsey makes no change to the atom and, as a result, the Ramsey fringe disappears. While, in the no entanglement case in Fig. 2(c), the interaction of $\alpha = 2\pi$ makes each atom return to $|+\rangle$, so the Ramsey fringe is maximally expected. Measured Ramsey fringes for $\alpha = \pi$ and 2π are respectively shown in Figs. 2(d) and 2(e). Measured fringe visibilities are plotted for six different distances in Fig. 2(f), in which the maximal and minimal visibilities correspond to $\alpha = 2\pi$ (c) and π (b), respectively. The Monte Carlo simulation estimates an entanglement fidelity of $\mathcal{F} = 0.59 \pm 0.11$ for the maximally entangled state $|\psi(\alpha = \pi)\rangle$ in Eq. (2).

The above scheme of pairwise entanglements works even in the presence of additional closer atoms, as long as they are properly placed. As an example, we consider a linear configuration of three atoms (A, B, and C), as shown

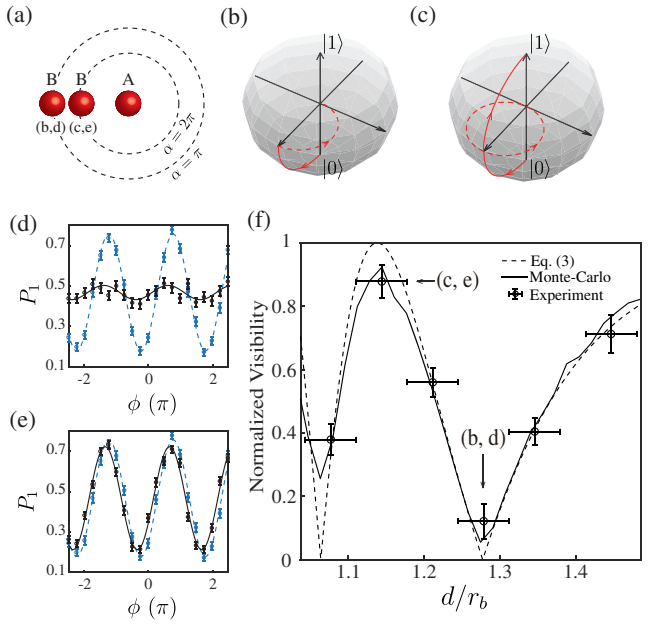

FIG. 2. (a) Two atoms A and B separated at a distance of either d_π for entanglement ($\alpha = \pi$) or $d_{2\pi}$ for no entanglement ($\alpha = 2\pi$). (b),(c) Quantum trajectories of each atom expected for (b) $\alpha = \pi$ and (c) $\alpha = 2\pi$. (d),(e) Measured Ramsey fringes, $P_1(\phi) = (P_1^A + P_1^B)/2$, for (d) $\alpha = \pi$ and (e) $\alpha = 2\pi$, compared with an isolated single-atom Ramsey fringe in blue. (f) Ramsey fringe visibilities measured at various distances compared with Monte Carlo simulation (solid line) and $|\cos(\tau C_6/2d^6)|$ (dashed line) of Eq. (3).

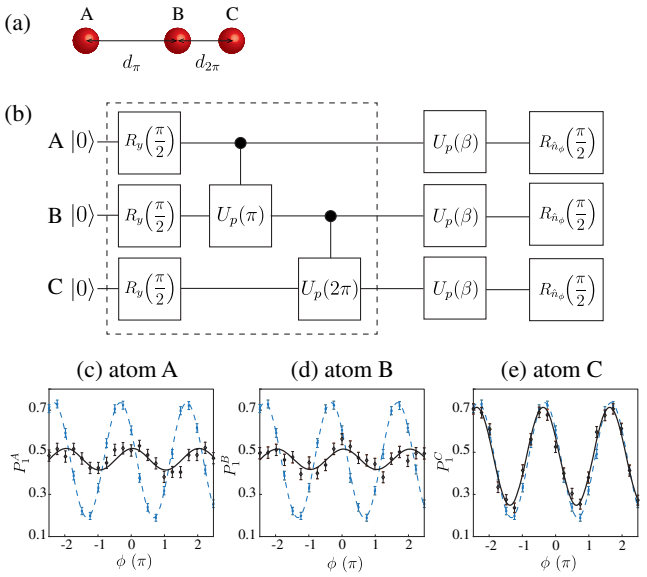

FIG. 3. (a) Linear arrangement of three atoms A, B, C with $d_{AB} = d_\pi$ and $d_{BC} = d_{2\pi}$. (b) An equivalent three-qubit quantum circuit (the two controlled gates commute). (c)–(e) Measured Ramsey fringes $P_1(\phi)$ of (c) atom A, (d) atom B, and (f) atom C, in comparison with that of an isolated single-atom in blue.

in Fig. 3(a), in which A and B are placed at $d_{AB} = d_\pi$ and the third atom C satisfies $d_{BC} = d_{2\pi}$. Then, $d_{AC} = d_\pi + d_{2\pi}$ approximates $\alpha_{AC} \approx 0$. The corresponding quantum circuit is drawn in Fig. 3(b), which includes a controlled π-phase gate between A and B, and a controlled 2π-phase gate between B and C. Ramsey measurements are shown in Figs. 3(c), 3(d), and 3(e) for the atoms A, B, and C, respectively. Entangled atoms, A and B, exhibit low fringe visibilities of 19% and 18%, respectively, while the unentangled atom C a high fringe visibility, closer to the case of an isolated single atom. Therefore, the result indicates that the remote pair (AB) can be entangled, while the closer pair (BC) is left unentangled.

In the final experiment, we consider an application of the weak coupling, for the generation of multipartite entanglements. For example, a system of three partially blockaded atoms (e.g., of $d_{AB}, d_{BC} < r_b < d_{AC}$ in the linear configuration), is never driven perfectly to the superatom state, $|W\rangle = (|100\rangle + |001\rangle + |010\rangle)/\sqrt{3}$, by a single resonant excitation of any pulse area Θ, i.e., $R(\Theta)|000\rangle \neq |W\rangle$. The system evolves also to unwanted leakage states $|W'\rangle = (|100\rangle + |001\rangle - 2|010\rangle)/\sqrt{6}$ and $|101\rangle$, due to the breaking of the Rydberg blockade of the AC pair [25]. In order to produce the $|W\rangle$ state of these three partially blockaded atoms, we adopt a coherent control method [26] that can destructively interfere with unwanted transitions and generate the target state with high fidelity. The first-order leakage state of the given partially blockade system is $|101\rangle$, so the given leakage transition, $|W\rangle \rightarrow |101\rangle$, can be undone by an additional phase-flipped transition, as illustrated in Fig. 4(a). Numerical optimization, performed for three atoms with $d_{AB} = d_{BC} = 0.66 r_b$ and $d_{AC} = 1.31 r_b$ (in this case $r_b = 8.96\ \mu$m and $\Omega = 2\pi \times 0.99$ MHz), predicts that the given leakage suppression [27] can be engineered, by two pulses with respective pulse areas $2\pi/3$ and $\pi/3$ (with respect to the three-atom collective Rabi frequency $\sqrt{3}\Omega$), and a time delay for the $|101\rangle$-state phase flipping, i.e., $|\psi_f\rangle = R_y(\pi/3)U_p^{AC}(\pi)R_y(2\pi/3)|000\rangle$. With this, all the leakages to unwanted singly excited and multiply excited states can be simultaneously suppressed, resulting in a high-fidelity $|W\rangle$-state generation of $|\langle W|\psi_f\rangle|^2 > 98\%$, as shown in Fig. 4(b). Experimental results are presented in Fig. 4(c), in which the probabilities of all singly excited states, $P_s = P_{100} + P_{010} + P_{001}$, and of all multiply excited states, $P_m = P_{110} + P_{011} + P_{101} + P_{111}$, are plotted with filled circles and squares, respectively, and compared with the corresponding single-pulse experiments (open circles and squares). The results of the given two-pulse coherent control scheme exhibit significant improvements at around $\Theta_{\text{total}} = \pi$, as predicted.

Our entanglement scheme (controlled phase gates in the weak-coupling regime) can be in principle generalized for N atoms, by utilizing individual atom addressing [28,29]. However, even in this case, maximally available N, estimated to be $N_{\max} \approx (2d_{\max}/d_{\min})^3$ in a three-dimensional array, is limited by two distance inequalities: (1) The

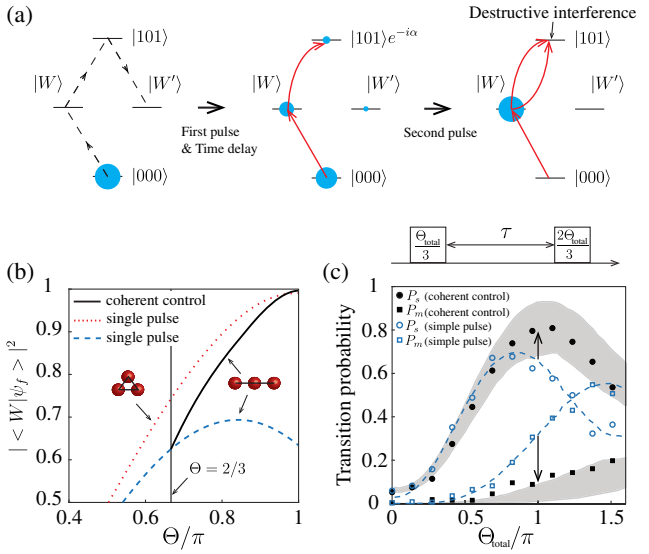

FIG. 4. (a) A coherent control scheme to generate the $|W\rangle$ state of partially blockaded ($d < r_b < 2d$) linear three atoms (see the text for details). (b) Transition probability $|\langle W|\psi_f(\Theta)\rangle|^2$ vs pulse area Θ, calculated for the coherent-control case (solid line) with $|\psi_f(\Theta)\rangle = R_y(\Theta - 2\pi/3)U_p^{AC}(\pi)R_y(2\pi/3)|000\rangle$ for $2\pi/3 < \Theta < \pi$. In comparison, single-pulse cases of fully blockaded triangular three atoms (dotted line) and the given linear three atoms (dashed line) are calculated with $|\psi_f\rangle = R_y(\Theta)|000\rangle$. (c) Experimentally measured probabilities $P_s(\Theta_{\text{total}})$ (of all singly excited states) and $P_m(\Theta_{\text{total}})$ (of all multiply excited states) in which the total pulse area, Θ_{total}, was varied from 0 to $3\pi/2$. State preparation and measurement errors of about 10% are taken into account and the shades represent central 50% sampling ranges of Monte Carlo simulations.

distance of nearest pairs needs to be larger than the Rydberg blockade radius, i.e., $d_{\min} = r_b$, and (2) the dephasing time T_2 limits the maximal distance, i.e., $d_{\max} = (C_6 T_2/\pi)^{1/6}$. Our current setup with $T_2 = 5.6$ μs allows $N_{\max} \approx 25$. It is expected that an increased dephasing time (e.g., $4 \times T_2$), by sideband cooling [30] and a pulse sequence such as spin echo [12], and a reduced blockade radius, by an increased Rabi oscillation frequency (e.g., $5 \times \Omega$), shall be able to achieve $N_{\max} > 100$.

Monte Carlo simulation modeling the current experiment estimates the entanglement fidelity of $\mathcal{F} = 0.59 \pm 0.11$ for the maximally entangled two-qubit state in Eq. (2). The fidelity errors are mostly from finite atom temperature and laser phase noise. The simulation also expects that sideband cooling [30] (below 3 μK) and laser stabilization [12] ($\Delta\phi < 0.01\pi$) would achieve $\mathcal{F} > 0.9$. It is noted that model A requires a longer gate time ($\tau \sim 1/U \gg 1/\Omega$) than conventional model B ($\tau \sim 1/\Omega$), which makes the entanglements achieved in the current scheme limited by the finite lifetime of the Rydberg state, not directly useful for quantum information processing. The short lifetime can be resolved, in future works, e.g., by encoding the qubit on two hyperfine ground levels [19], with one of the two momentarily excited by a π pulse (in contrast to the $\pi/2$ pulse used in this work) to accumulate the interaction phase. It is also noted that the interaction phase of a doubly exited Rydberg state is sensitive to the interatomic distance ($\Delta\alpha/\alpha = 6\Delta d/d$), so the entanglement method based on model A requires accurate control of d. In our experiments, the repulsive force between Rydberg atoms is negligible; atom displacement by the repulsive force during a controlled π-phase gate is estimated to be less than 8 nm. The distance errors mainly come from the atom temperature that causes atom position jitters about 0.13 μm. Numerical data fitting of experimental data, taking into account the above errors in Monte Carlo simulation, estimates $\Delta d \simeq 0.14$ μm and $\Delta\alpha/\alpha \simeq 7\%$.

In summary, we have presented experimental demonstration of the Rydberg-atom entanglement in the weak coupling regime. Our experiments are based on model A of Rydberg-atom two-qubit gate proposals in Ref. [19], enabling long distance entanglements and multipulse coherent control methods. The current scheme requires longer gate time and more accuracy of the interatomic distance than the conventional method using Rydberg blockade effect. Monte Carlo simulation estimates the current experiment achieves the entanglement fidelity of $\mathcal{F} = 0.59 \pm 0.11$, which can be further improved by using long-lived hyperfine states, sideband cooling, and laser frequency stabilization. The entanglement method demonstrated in this work could be of particular importance in dealing with entanglements of massive qubit systems, e.g., one-way quantum computing with geometrically imprinted cluster states [31].

The authors thank the anonymous referees for valuable comments and Andrew Byun for fruitful discussion. This research was supported by Samsung Science and Technology Foundation [SSTF-BA1301-52] and National Research Foundation of Korea [NRF-2017R1E1A1A01074307].

*jwahn@kaist.ac.kr

[1] R. Horodecki, P. Horodecki, M. Horodecki, and K. Horodecki, Quantum entanglement, Rev. Mod. Phys. **81**, 865 (2009).
[2] R. Islam, R. Ma, P. M. Preiss, M. E. Tai, A. Lukin, M. Rispoli, and M. Greiner, Measuring entanglement entropy in a quantum many-body system, Nature (London) **528**, 77 (2015).
[3] H. Bernien, S. Schwartz, A. Keesling, H. Levine, A. Omran, H. Pichler, S. Choi, A. S. Zibrov, M. Endres, M. Greiner, V. Vuletić, and M. D. Lukin, Probing many-body dynamics on a 51-atom quantum simulator, Nature (London) **551**, 579 (2017).
[4] H. Kim, Y. J. Park, K. Kim, H.-S. Sim, and J. Ahn, Detailed Balance of Thermalization Dynamics in Rydberg-Atom Quantum Simulators, Phys. Rev. Lett. **120**, 180502 (2018).
[5] M. A. Nielsen and I. L. Chuang, *Quantum Computation and Quantum Information* (Cambridge University Press, Cambridge, England, 2010).

[6] C. L. Degen, F. Reinhard, and P. Cappellaro, Quantum sensing, Rev. Mod. Phys. **89**, 035002 (2017).
[7] R. Ursin, F. Tiefenbacher, T. Schmitt-manderbach, H. Weier, T. Scheidl, M. Lindenthal, B. Blauensteiner, T. Jennewein, J. Perdigues, P. Trojek, B. Omer, M. Furst, M. Meyenburg, J. Rarity, Z. Sodnik, C. Barbieri, H. Weinfurter, and A. Zeilinger, Entanglement-based quantum communication over 144 km, Nat. Phys. **3**, 481 (2007).
[8] P. G. Kwiat, K. Mattle, H. Weinfurter, A. Zeilinger, A. V. Sergienko, and Y. Shih, New High-Intensity Source of Polarization-Entangled Photon Pairs, Phys. Rev. Lett. **75**, 4337 (1995).
[9] T. Wilk, A. Gaëtan, C. Evellin, J. Wolters, Y. Miroshnychenko, P. Grangier, and A. Browaeys, Entanglement of Two Individual Neutral Atoms Using Rydberg Blockade, Phys. Rev. Lett. **104**, 010502 (2010).
[10] L. Isenhower, E. Urban, X. L. Zhang, A. T. Gill, T. Henage, T. A. Johnson, T. G. Walker, and M. Saffman, Demonstration of a Neutral Atom Controlled-NOT Quantum Gate, Phys. Rev. Lett. **104**, 010503 (2010).
[11] Y.-Y. Jau, A. M. Hankin, T. Keating, I. H. Deutsch, and G. W. Biedermann, Entangling atomic spins with a Rydberg-dressed spin-flip blockade, Nat. Phys. **12**, 71 (2016).
[12] H. Levine, A. Keesling, A. Omran, H. Bernien, S. Schwartz, A. S. Zibrov, M. Endres, M. Greiner, V. Vuletić, and M. D. Lukin, High-Fidelity Control and Entanglement of Rydberg-Atom Qubits, Phys. Rev. Lett. **121**, 123603 (2018).
[13] Q. A. Turchette, C. S. Wood, B. E. King, C. J. Myatt, D. Leibfried, W. M. Itano, C. Monroe, and D. J. Wineland, Deterministic Entanglement of Two Trapped Ions, Phys. Rev. Lett. **81**, 3631 (1998).
[14] J. H. Plantenberg, P. C. de Groot, C. J. P. M. Harmans, and J. E. Mooij, Demonstration of controlled-NOT quantum gates on a pair of superconducting quantum bits, Nature (London) **447**, 836 (2007).
[15] P. Neumann, N. Mizuochi, F. Rempp, P. Hemmer, H. Watanabe, S. Yamasaki, V. Jacques, T. Gaebel, F. Jelezko, and J. Wrachtrup, Multipartite entanglement among single spins in diamond, Science **320**, 1326 (2008).
[16] J. I. Cirac and P. Zoller, Quantum Computations with Cold Trapped Ions, Phys. Rev. Lett. **74**, 4091 (1995).
[17] F. Schmidt-Kaler, H. Häffner, M. Riebe, S. Gulde, G. P. T. Lancaster, T. Deuschle, C. Becher, C. F. Roos, J. Eschner, and R. Blatt, Realization of the Cirac-Zoller controlled-NOT quantum gate, Nature (London) **422**, 408 (2003).
[18] A. J. Berkley, H. Xu, R. C. Ramos, M. A. Gubrud, F. W. Strauch, P. R. Johnson, J. R. Anderson, A. J. Dragt, C. J. Lobb, and F. C. Wellstood, Entangled macroscopic quantum states in two superconducting qubits, Science **300**, 1548 (2003).
[19] D. Jaksch, J. I. Cirac, P. Zoller, S. L. Rolston, R. Cote, and M. D. Lukin, Fast Quantum Gates for Neutral Atoms, Phys. Rev. Lett. **85**, 2208 (2000).
[20] A. Widera, O. Mandel, M. Greiner, S. Kreim, T. W. Hänsch, and I. Bloch, Entanglement Interferometry for Precision Measurement of Atomic Scattering Properties, Phys. Rev. Lett. **92**, 160406 (2004).
[21] H. Kim, W. Lee, H. Lee, H. Jo, Y. Song, and J. Ahn, In situ single-atom array synthesis using dynamic holographic optical tweezers, Nat. Commun. **7**, 13317 (2016).
[22] W. Lee, M. Kim, H. Jo, Y. Song, and J. Ahn, Coherent and dissipative dynamics of entangled few-body systems of Rydberg atoms, Phys. Rev. A **99**, 043404 (2019).
[23] S. Weber, C. Tresp, H. Menke, A. Urvoy, O. Firstenberg, H. P. Büchler, and S. Hofferberth, Tutorial: Calculation of Rydberg interaction potentials, J. Phys. B **50**, 133001 (2017).
[24] C. Tuchendler, A. M. Lance, A. Browaeys, Y. R. P. Sortais, and P. Grangier, Energy distribution and cooling of a single atom in an optical tweezer, Phys. Rev. A **78**, 033425 (2008).
[25] D. Barredo, S. Ravets, H. Labuhn, L. Béguin, A. Vernier, F. Nogrette, T. Lahaye, and A. Browaeys, Demonstration of a Strong Rydberg Blockade in Three-Atom Systems with Anisotropic Interactions, Phys. Rev. Lett. **112**, 183002 (2014).
[26] C. Brif, R. Chakrabarti, and H. Rabitz, Control of quantum phenomena: past, present and future, New J. Phys. **12**, 075008 (2010).
[27] H. Jo, Y. Song, and J. Ahn, Qubit leakage suppression by ultrafast composite pulses, Opt. Express **27**, 3944 (2019).
[28] H. Labuhn, S. Ravets, D. Barredo, L. Béguin, F. Nogrette, T. Lahaye, and A. Browaeys, Single-atom addressing in microtraps for quantum-state engineering using Rydberg atoms, Phys. Rev. A **90**, 023415 (2014).
[29] Y. Wang, X. Zhang, T. A. Corcovilos, A. Kumar, and D. S. Weiss, Coherent Addressing of Individual Neutral Atoms in a 3D Optical Lattice, Phys. Rev. Lett. **115**, 043003 (2015).
[30] A. M. Kaufman, B. J. Lester, and C. A. Regal, Cooling a Single Atom in an Optical Tweezer to its Quantum Ground State, Phys. Rev. X **2**, 041014 (2012).
[31] R. Raussendorf and H. J. Briegel, A One-Way Quantum Computer, Phys. Rev. Lett. **86**, 5188 (2001).